IIETA International Information and Engineering Technology Association
Advancing the World of Information and Engineering

Ingénierie des Systèmes d'Information
Vol. 31, No. 6, June, 2026, pp. 1803-1810
Journal homepage: http://iieta.org/journals/isi

Optimal Rank Selection for Image Compression Using Singular Value Decomposition Based on Singular Value Analysis

Aqeel Majeed Breesam[1*], Mohammed Q. Mohammed[2], Ward Ahmed Al-Hussein[3], Hadeel Talib Mangi[4]

[1] Institute of Medical Technology/Baghdad, Middle Technical University, Baghdad 10001, Iraq
[2] Department of Informatics Systems Management, University of Information Technology and Communications, Baghdad 10001, Iraq
[3] Information Technology Management Department, Technical College of Management, Middle Technical University, Baghdad 10001, Iraq
[4] Computer Science and Information Technology Department, College of Science, University of Hilla, Babylon 51011, Iraq

Corresponding Author Email: aqeelmajeed@mtu.edu.iq

https://doi.org/10.18280/isi.310603

Received: 24 March 2026
Revised: 20 May 2026
Accepted: 28 May 2026
Available online: 30 June 2026

Keywords:
image compression, singular value decomposition, low-rank approximation, singular value truncation, rank selection, mean squared error, peak signal-to-noise ratio

ABSTRACT

Image compression plays an important role in reducing storage requirements and improving transmission efficiency in digital image processing applications. Singular value decomposition (SVD) provides an effective low-rank approximation technique by decomposing an image matrix into two orthogonal matrices and a diagonal singular-value matrix, thereby enabling image reconstruction with fewer singular components while preserving essential visual information. This study investigated the influence of singular value selection on the compression performance of images with relatively high pixel-intensity variation. Different truncation ranks were evaluated to determine the relationship between size reduction (SR) and reconstructed-image quality. The performance of the reconstructed images was assessed using mean squared error (MSE) and peak signal-to-noise ratio (PSNR). The results demonstrated that selecting an appropriate number of singular values was critical for achieving a balance between storage reduction and image fidelity. The selected truncation rank was $R = 20$, which achieved a size reduction of 20% while maintaining a PSNR of 32.2 dB. The findings indicated that SVD-based rank reduction could reduce image-storage requirements with limited degradation in reconstructed-image quality.

1. INTRODUCTION

Digital images are widely used throughout the fields of communication, medicine, remote sensing, security, entertainment and many other areas of computer systems. The huge growth in the quantity and resolution of digital images has led to the search for efficient storage and transmission systems. Image compression can be defined as the process of representing image data with a minimum number of bits with controlled degradation in the reconstructed image [1, 2]. Thus, an image compression method should be optimal in terms of storage, communication requirement, computational complexity and quality of the reconstructed image.

Remote-computing environments provide for transmission of extensive amounts of multimedia data and allow deployment of large storage and retrieval systems [3]. High-quality images, however, demand high-memory capacity and communication bandwidth. Digital images, furthermore, has storage-space redundancy since the intensities of adjacent pixels tend to be similar [4, 5]. Digital-image-compression algorithms utilize this redundancy to decrease storage space needed and aim at be limiting the loss of quality in reconstructed Images [6].

One of the most prevalent methods for image compression is the Joint Photographic Experts Group (JPEG) standard. The JPEG method uses the discrete cosine transform (DCT) to gather image information into a small collection of transform coefficients. There are many other compression approaches such as wavelet-based methods, matrix-factorization based methods and learning-based models [7]. For instance, singular value decomposition (SVD) within the matrix-factorization based methods is used to give a low-rank approximation of the image matrix by keeping just the leading singular terms.

The success of an SVD-based compression relies mainly on the low-rank nature of the image data and the magnitude by which the singular values decay [8]. If majority of the image information can be captured by the leading singular values, then the image can be recovered using a fewer number of components with a minimal loss of visual information. The smaller the truncation rank, the greater the compression (storage saving), but the more the reconstruction error; the larger, the better the image quality, but at the expense of more storage space.

Data representation and transmission: SVD is also used for data representation and transmission since it condenses the dimension while retaining the most significant overall structure information [9]. If the image is then transmitted in its compressed form this allows a simultaneous reduction in storage, communication time and required bandwidth in long-distance communication systems [10, 11]. There is, however, still the issue of choosing a suitable truncation rank, as a static rank value will provide fluctuating image storage compression and image reconstruction quality between images of dissimilar overall structure.

This paper explores how the truncation rank influences SVD compression of images. Mean squared error (MSE), peak signal-to-noise ratio (PSNR) and reduction in file size are used to compare a number of different values for the rank. It seeks to determine a suitable rank that offers a compromise between quality of the reconstructed image, and size reduction.

The rest of the paper is organized as below: Section 2 presents the related work. Section 3 describes the methodology. Sections 4 presents and discusses the experimental results. Section 5 summarizes the main conclusions and limitations.

2. RELATED WORKS

Ahmed [12] presented an adaptive strategy for selecting singular-values in SVD-based image compression in order to maintain perceptually relevant edges. Rather than discarding the same percentage of singular values in all blocks, a percentage ranging from 5 to 30% was chosen based on the variance of the block. The higher the variance of a block, the more likely it was to contain strong edges and thus the lower the discard percentage were. For the tested car image, the method achieved a PSNR of 32.028 dB and a compression ratio of 3.405, compared with 30.5994 dB and 3.510, respectively, for the fixed 30% strategy. The results indicated improved edge preservation with a limited change in compression performance.

Al-Obaidi and Ahmed [13] investigated SVD-based image compression as a means of reducing image redundancy and improving storage and transmission efficiency. Their methodology consisted of two main stages: computation of the SVD and reconstruction of the image using a reduced matrix rank. Their experimental results showed that the selected rank strongly affected both compression efficiency and reconstructed-image quality. PSNR and compression ratio were used as the principal performance measures.

Taj et al. [14] proposed an SVD-based zero-watermarking method for protecting the integrity of medical images without modifying diagnostically important image content. Speeded-up robust features were used for feature extraction, and SVD was applied in the frequency-domain representation. The method was evaluated under Gaussian noise, JPEG compression, cropping, rotation, and other distortions. The reported normalized-correlation and PSNR results demonstrated strong robustness under the tested attacks.

Kumar and Parmar [15] reviewed several approaches to medical-image compression and discussed their ability to address storage and bandwidth limitations. They identified compression ratio as an important performance measure and summarized the principal advantages and disadvantages of the reviewed methods. However, because the study did not provide a unified experimental comparison, its conclusions regarding relative compression performance were primarily qualitative.

Latreche et al. [16] proposed a medical-image watermarking method that combined the lifting wavelet transform, Hessenberg decomposition, SVD, and chaotic encryption based on the logistic map. The medical image was first decomposed using a multilevel lifting wavelet transform and Hessenberg decomposition. The watermark was then scrambled using a chaotic sequence and embedded in the SVD domain with an adaptively selected scaling factor. The method achieved high imperceptibility and PSNR values above 45 dB and remained robust under several image-processing attacks.

Liu et al. [17] developed an SVD-based color-image watermarking scheme in which each image block was represented as a two-dimensional matrix and decomposed using SVD. The watermark information was embedded by modifying the first singular value. A generalized regression neural network was trained to estimate the original singular values, eliminating the need to transmit them separately during watermark recovery. Adaptive embedding strength was used to improve the balance between watermark imperceptibility and robustness. The method showed resistance to filtering, JPEG compression, and other standard attacks.

Sundara Rajan and Fred [18] combined run-length encoding with an optimized discrete wavelet transform for compound-image compression. Their method included preprocessing and wavelet-coefficient optimization to improve compression performance and reduce computation time. Optimization of the Haar-wavelet coefficients produced favorable results for the tested compound images. However, the method was not evaluated using remote-sensing images.

Asokan et al. [19] reviewed image-processing techniques for satellite-image analysis and historical-map classification. Their study compared the advantages and limitations of several processing methods and discussed the challenges associated with complex satellite imagery. They saw that deciding on an image-processing approach depends on the type of input-image, the amount of detail, and others. They also realized that machine-learning algorithms hold the ability to learn discriminative image representations.

Barbhuiya et al. [20] compared methods for compression of JPEG and PNG color images, based on DCT and DWT. In their implementation of DWT color images were reduced to greyscale prior to compression. The authors provided a comparison between the two transforms for the conditions of their experiment.

Cho and Jeon [21] discussed SVD compression of X-ray and magnetic-resonance medical images. Their work explained criteria for choosing a compression threshold based on recognized image-quality metrics. Their proposed method aimed to optimize the tradeoff between data compression and quality of reconstructed image.

Together, the literature shows the extensive application of SVD for image compression, watermarking, and reduction of dimensionality. The literature also indicates the strong dependence of compression results to the number of singular components kept. This research, thus, investigates a transparent rank-selection criterion for SVD-only image compression and explores the relationships among the truncation rank, the reconstructed image quality, and the amount of data storage reduction.

3. METHOD

The SVD based compression is very efficient when there is a high amount of information in the first few singular values.

In this case the image can be represented with a lower rank matrix while preserving its dominant feature: the spatial location. The suitability of this approximation is determined more by the number and decay of the singular values than pixel-intensity standard deviation. More specifically, images with relatively broad variation in intensity were used in this work in order to explore the relationship among the truncation rank, storage reduction and quality of reconstruction.

Figure 1 presents the four test images on which the tests were based: this is a man image taken from the database Faces94 a woman image, an elephant image and the Kodak image kodim23. Their original file sizes were 36, 40.9, 48.1, and 40 KB, respectively. The corresponding pixel dimensions were 180 × 200, 352 × 440, 660 × 371, and 768 × 512 pixels, respectively. File size and image resolution are reported separately as kilobytes provides information regarding storage size rather than spatial resolution.

Each image was converted to grayscale and represented as an $m \times n$ matrix A. The man image had dimensions of 180 × 200 pixels. As seen in Figure 2, the flow of experiment involved image pre-processing, SVD, rank-R truncation, image reconstruction and performance evaluation. Reconstructions were generated using the tested rank values, and their quality was assessed using MSE and PSNR. Storage performance was evaluated using percentage size reduction.

The selected operating rank was defined as the smallest tested value of R that produced an MSE below 40 for the man image. This criterion was used to identify a practical balance between storage reduction and reconstruction quality. The same selected rank was then evaluated using the remaining test images.

The experiments were performed using MATLAB R2018a under Windows 10 on a computer equipped with 32 GB of RAM and an Intel Core i5 processor operating at 4.7 GHz.

Figure 1. Test images used in the experiments

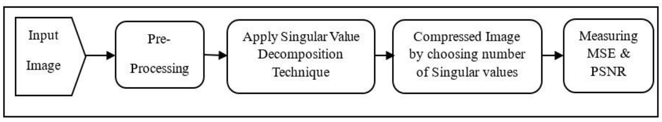

Figure 2. Block diagram of the proposed singular value decomposition (SVD)-based compression framework

3.1 Image preprocessing

Digital images may be affected by noise during acquisition, processing, transmission, compression, or storage. Salt-and-pepper noise appears as isolated dark and bright pixels and can adversely affect subsequent image processing. In this study, a median filter was applied as a preprocessing step to reduce impulse noise before SVD compression.

A median filter is a nonlinear spatial filter that replaces the central pixel value with the median of the intensity values within a local neighborhood. Unlike a mean filter, it does not replace the pixel with the arithmetic average of neighboring values. Because the median is less sensitive to extreme values, the filter can suppress impulse noise while preserving edges more effectively than many linear smoothing filters. A 3 × 3 median-filter window was used in the experiments. Figure 3 summarizes the preprocessing procedure.

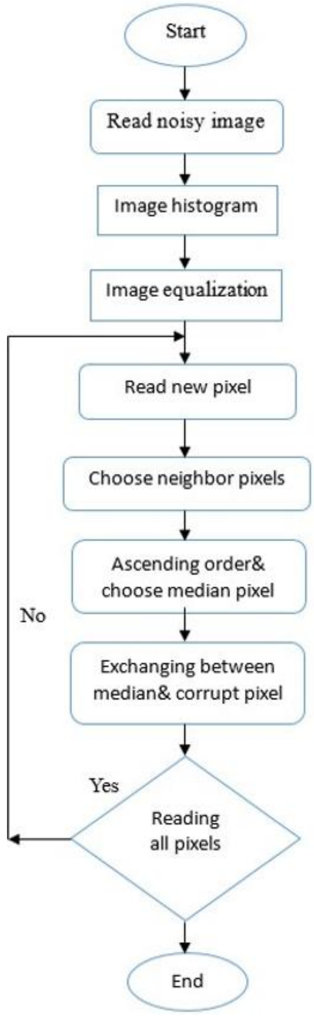

Figure 3. Flowchart of median-filter preprocessing

3.2 Singular value decomposition

Let $A \in \mathbb{R}^{m \times n}$ denote an image matrix with m rows and $n$columns. The singular value decomposition of A is

$$A = U\Sigma V^T \tag{1}$$

where, $U \in \mathbb{R}^{m \times m}$ and $V \in \mathbb{R}^{n \times n}$ are orthogonal matrices, and $\Sigma \in \mathbb{R}^{m \times n}$ is a rectangular diagonal matrix containing the singular values of A. The orthogonality conditions are

$$U^T U = I_m \tag{2}$$

$$V^T V = I_n \tag{3}$$

The singular-value matrix can be written as

$$\Sigma = \begin{bmatrix} \sigma_1 & 0 & \cdots & 0 \\ 0 & \sigma_2 & \cdots & 0 \\ \vdots & \vdots & \ddots & \vdots \\ 0 & 0 & \cdots & \sigma_p \end{bmatrix} \tag{4}$$

where, $p = \min(m, n)$ and $\sigma_1 \geq \sigma_2 \geq \cdots \geq \sigma_p \geq 0$.

To obtain a rank-R approximation, only the first R singular values and their corresponding singular vectors are retained:

$$A_R = U_R \Sigma_R V_R^T = \sum_{i=1}^{R} \sigma_i \, u_i v_i^T \tag{5}$$

The value R is referred to as the truncation rank. A smaller rank requires fewer retained components but generally produces a larger reconstruction error. A larger rank preserves more image information but requires additional storage.

3.3 Performance measures

The quality of each reconstructed image was evaluated using MSE and PSNR. Storage performance was evaluated using percentage size reduction.

Let $X(i,j)$ and $Y(i,j)$ denote the pixel values of the original and reconstructed images, respectively. For an image of size $m \times n$, MSE is defined as

$$\text{MSE} = \frac{1}{mn} \sum_{i=1}^{m} \sum_{j=1}^{n} [X(i,j) - Y(i,j)]^2 \tag{6}$$

A lower MSE indicates that the reconstructed image is closer to the original image. MSE is reported without a decibel unit.

PSNR is defined as

$$\text{PSNR} = 10\log_{10}\left(\frac{MAX_I^2}{\text{MSE}}\right) \tag{7}$$

where, MAX_I is the maximum possible pixel value. For an 8-bit image, $MAX_I = 255$. PSNR is expressed in decibels, and a higher PSNR generally indicates better reconstruction quality. Let F_{original} and $F_{\text{compressed}}$ denote the original and compressed file sizes, respectively. Percentage size reduction is calculated as

$$SR(\%) = \frac{F_{\text{original}} - F_{\text{compressed}}}{F_{\text{original}}} \times 100 \tag{8}$$

A higher value of SR indicates a larger reduction in storage requirements. The original and reconstructed images were saved in JPEG format using identical spatial dimensions, grayscale representation, and encoding settings. Their file sizes were measured in kilobytes and used to calculate percentage size reduction.

4. RESULT AND DISCUSSION

Figure 4 presents the man image reconstructed with various ranks of truncation as noted. More singular components were kept as R increased, thus improving the quality of the reconstructed image. At very low ranks, the reconstructed image failed to capture the details and was blurred. With increased rank, the reconstructed image approached the original image.

Figure 5 shows MSE versus the truncation rank. The MSE is smaller for larger R because the more singular components are included in the approximation. Reconstructions with $R < 20$ had an MSE of 40 or greater and showed noticeable visual degradation. At $R = 20$, the MSE decreased to 38.5. This value was below the predefined threshold of 40 and was therefore considered acceptable under the criterion used in this study.

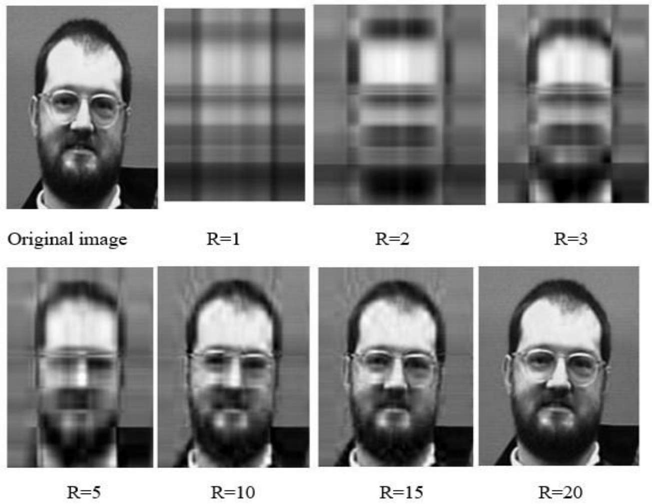

Figure 4. Man image: (a) original image; reconstructed images at (b) $R = 1$, (c) $R = 2$, (d) $R = 3$, (e) $R = 5$, (f) $R = 10$, (g) $R = 15$, and (h) $R = 20$

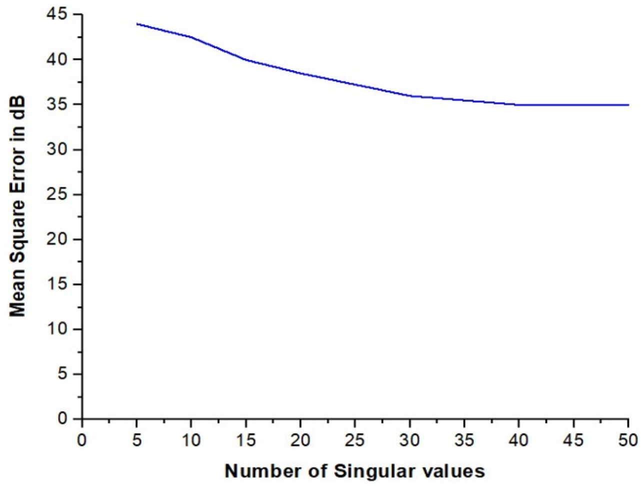

Figure 5. Mean squared error versus truncation rank R

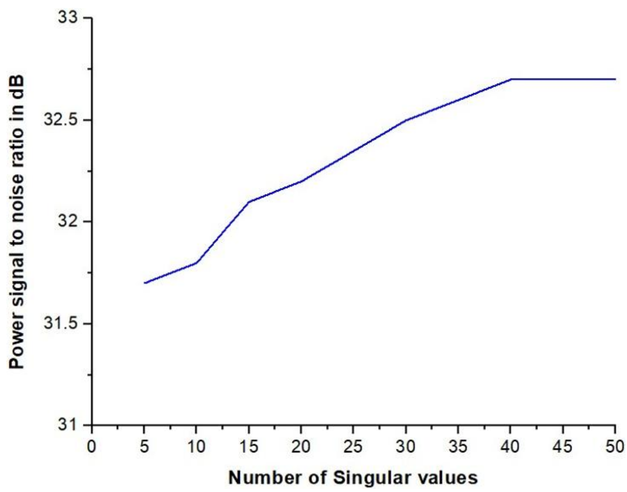

Figure 6. Peak signal-to-noise ratio versus truncation rank R

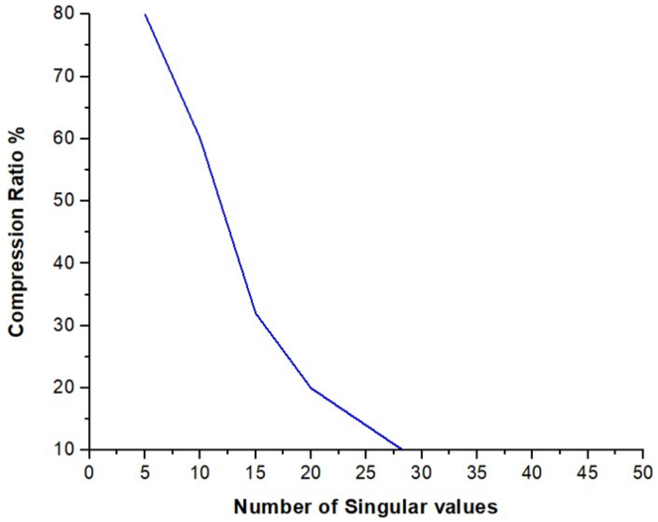

Figure 7. Percentage size reduction versus truncation rank R

Table 1. Compression performance for the man image at different truncation ranks

Truncation Rank, R	Size Reduction, SR (%)	Mean Squared Error	Peak Signal-to-Noise Ratio (dB)
5	80	44.0	31.7
10	60	42.5	31.8
15	32	40.0	32.1
20	20	38.5	32.2
30	8	36.0	32.5
40	4	35.0	32.7
50	3	35.0	32.7

Figure 6 shows that PSNR increased as the truncation rank increased. The PSNR was 31.7 dB at $R = 5$, 31.8 dB at $R = 10$, 32.1 dB at $R = 15$, and 32.2 dB at $R = 20$. Further increases in rank produced only modest PSNR improvements, reaching 32.7 dB at $R = 40$ and $R = 50$.

Figure 7 and Table 1 illustrate the trade-off between storage reduction and image quality. Lower ranks produced greater size reductions but also resulted in higher MSE and lower PSNR. Higher ranks improved image quality but reduced the storage saving. At $R = 20$, the method provided a 20% file-size reduction, an MSE of 38.5, and a PSNR of 32.2 dB. Among the tested values, $R = 20$ was the smallest rank that satisfied the MSE threshold. It was therefore selected as the operating rank for the subsequent experiments.

The rank selection is application-dependent. High visual fidelity applications may have to adopt a truncation ranker than 20, while storage-limited would be more willing to use a lower rank trading for more error in the reconstruction.

In this work, R = 20 was chosen as the lowest tested rank that meets the given MSE standard. That implies for this work images, R = 20 is the selected operating point rather than stand for any other images.

Figures 8–10 display the reconstructed woman, elephant, and Kodak images at the following truncation ranks 5, 10, 15, and 20. For each of the three images, the amount of visual information increased with the rank. The low-rank reconstructions had soft edges and blurry regions, while the reconstructions at R = 20 maintained much of the structure and detail seen in the original image.

According to Table 2, the file size of the woman image decreased from 40.9 to 32.7 KB, corresponding to a size reduction of approximately 20%. Similarly, the file size of the elephant image decreased from 48.1 to 38.5 KB, corresponding to a size reduction of approximately 20%. The file size of the Kodak image decreased from 40.0 to 25.0 KB, corresponding to a size reduction of 37.5%.

These results showed that truncated SVD reduced the storage requirements of the tested images while retaining their dominant visual structures. However, some information was lost because the method is lossy. Excessive rank reduction increased blur and removed fine details. The truncation rank must therefore be selected according to the quality requirements of the intended application.

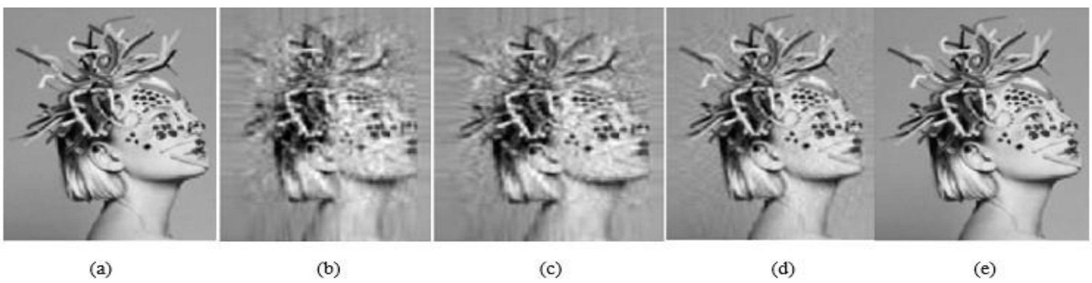

Figure 8. Woman image: (a) original image; reconstructed images at (b) $R = 5$, (c) $R = 10$, (d) $R = 15$, and (e) $R = 20$

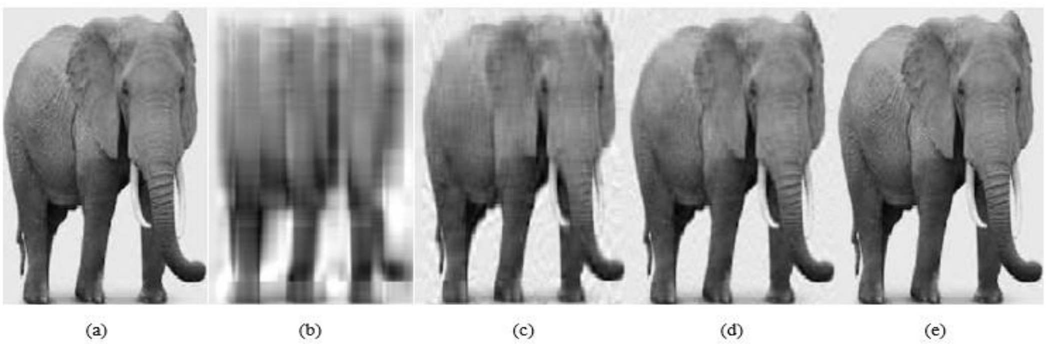

Figure 9. Elephant image: (a) original image; reconstructed images at (b) $R = 5$, (c) $R = 10$, (d) $R = 15$, and (e) $R = 20$

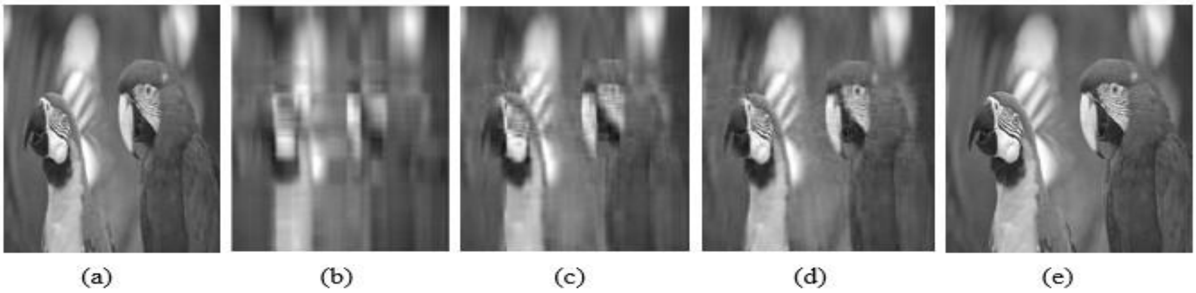

Figure 10. Kodak kodim23 image: (a) original image; reconstructed images at (b) $R = 5$, (c) $R = 10$, (d) $R = 15$, and (e) $R = 20$)

Table 2. Comparison of compressed file sizes and percentage size reductions

Image	Method	Original File Size (KB)	Resolution (pixels)	Compressed File Size (KB)	Size Reduction (SR) (%)
Faces94 man image	Proposed method	36.0	180 × 200	28.8	20.0
Woman image	Proposed method	40.9	352 × 440	32.7	20.0
Elephant image	Proposed method	48.1	660 × 371	38.5	20.0
Kodak image (kodim23)	Proposed method	40.0	768 × 512	25.0	37.5
Woman image	Ref. [22]	40.9	352 × 440	28.0	31.5
Elephant image	Ref. [22]	48.1	660 × 371	33.5	30.4
Woman image	Ref. [23]	40.9	352 × 440	30.0	26.7
Elephant image	Ref. [23]	48.1	660 × 371	38.0	21.0
Woman image	Ref. [24]	40.9	352 × 440	35.0	14.4
Elephant image	Ref. [24]	48.1	660 × 371	42.0	12.7
Woman image	Ref. [25]	40.9	352 × 440	39.0	4.6
Elephant image	Ref. [25]	48.1	660 × 371	45.0	6.4

Table 3. Peak signal-to-noise ratio (PSNR) values reported in previous studies and the present study

Reference	Year	Database	Algorithm Used	PSNR (dB)
[26]	2025	Medical images	DWT + DCT + SVD	35.2–38.4
[27]	2026	Different host images	HD + DWT + SVD	Up to 49
[28]	2025	Different medical images	DWT + HMD + SVD	49
[29]	2025	ColoR images	HD + SVD + DWT	46.4928
[30]	2024	Boat images	SVD	24.64
[31]	2022	Different images	SVD	24.2
Present study	2026	Different images	SVD	32.2

Note: SVD: singular value decomposition; DCT: discrete cosine transform; DWT: discrete wavelet transform; HD: Hessenberg decomposition; HMD: Hessenberg matrix decomposition.

Table 2 compares the file-size reductions obtained using the proposed method with those reported for previous methods. Under the current experimental settings, the proposed method achieved a 20% size reduction for the woman and elephant images. Compression results should be compared only when the same source images, file formats, quality requirements, and size-measurement procedures are used. Differences in these conditions can substantially affect both compressed file size and reconstructed-image quality. Therefore, the comparison is interpreted as indicative rather than conclusive.

Table 3 summarizes PSNR values reported in several previous studies. The hybrid DWT-, DCT-, HD-, and SVD-based methods reported higher PSNR values than the SVD-only approach evaluated in the present study. However, these values are not directly comparable because the studies used different datasets, image-processing objectives, embedding or compression settings, and evaluation protocols. In particular, several cited studies address image watermarking rather than image compression. The PSNR of 32.2 dB obtained in the present study should therefore be interpreted within the current dataset and experimental configuration rather than as a direct performance ranking against all methods listed in Table 3.

The evaluation was limited to four test images and one SVD-based compression configuration. While the introduced rank seems to be able to give a reasonable tradeoff of reconstruction error to compression for the images tested, the same value of may not have similar performance on images with very different sizes, textures, levels of noise, singular-value distributions, etc. Runtime, memory usage and statistical variance were not examined, either. These problems should be overcome by testing on larger sets of standard images and by comparison experiments performed in the same test environment.

5. CONCLUSIONS

In this experiment we explored the effect of the truncation rank on the use of SVD for image compression. Clearly there was a balance to be maintained between reduction in storage, and in the quality of reconstruction. Smaller ranks preserved fewer singular values, and achieved higher reductions in storage, albeit at the cost of an almost invariably blurrier image, and a higher residual error of reconstruction. Larger ranks maintained a greater fidelity of image, but with a greater storage requirement.

Of all the provided ranks, $R = 20$, was the minimum that met the set MSE rule for the man image, while maintaining a reasonable compromise between file-size reduction and quality of the reconstructed-image. This result emphasizes the need for choosing the rank according to a strict quality measure, not arbitrarily fixed at some value. Nevertheless, it is inappropriate to regard this rank as absolute optimal, as the suitable rank depends on image structure and application considerations.

The experiments were only conducted with four images and one preprocess/compress setup. Many tasks remain for further investigations including testing on the more extensive standard image sets, quantifying time and space consumed, and contrasting SVD with DCT-based and DWT-based compression, JPEG, and hybrid approaches with the same set of experimental parameters. Strategies for automating rank-choice could also be explored if the function to optimize, the parameters, and the optimization method were completely specified.

REFERENCES

[1] Breesam, A.M., Hussein, Y.M., Mohammed, M.J. (2024). Fractal compression of digital image processing. AIP Conference Proceedings, 3051(1): 040010. https://doi.org/10.1063/5.0191578

[2] Breesam, A.M., Zalzala, A.M., Najjar, E. (2024). Walsh transform-based image compression for less memory usage and high speed transfer. Majlesi Journal of Electrical Engineering, 18(1): 137-143. https://doi.org/10.30486/mjee.2023.1996722.1267

[3] Zhang, Y., Xu, B., Zhou, N. (2017). A novel image compression–encryption hybrid algorithm based on the analysis sparse representation. Optics Communications, 392: 223-233. https://doi.org/10.1016/j.optcom.2017.01.061

[4] Kapoor, A., Dhir, R. (2011). Image compression using fast 2-D DCT technique. International Journal on Computer Science and Engineering, 3(6): 2415-2419.

[5] Mangi, H.T., Ali, S.A., Jawad, M.J. (2023). Enhancing of coverless image steganography capacity based on image block features. Telecommunication Computing Electronics and Control, 21(6): 1364-1372. https://doi.org/10.12928/telkomnika.v21i6.24816

[6] Mounika, K., Lakshmi, D.S.N., Alekya, K., Tagore, M.R.N. (2015). SVD based image compression. International Journal of Engineering Research and General Science, 3(2): 1-5.

[7] Zhao, J., An, P., Huang, X., Yang, C., Shen, L. (2019). Light field image compression via CNN-based EPI super-resolution and decoder-side quality enhancement. IEEE Access, 7: 135982-135998. https://doi.org/10.1109/ACCESS.2019.2930644

[8] Venkataseshaiah, M.B., KN, M.R., Michahial, S. (2016). Image compression using singular value decomposition. Image, 5(12): 208-211. http://doi.org/10.17148/IJARCCE.2016.51246

[9] Fakhar, A.G.S., Saad, M.H., Fauzan, K.A., Affendi, H.R., Aidil, A.M. (2019). Development of portable automatic number plate recognition (ANPR) system on Raspberry Pi. International Journal of Electrical and Computer Engineering, 9(3): 1805-1813. https://doi.org/10.11591/ijece.v9i3.pp1805-1813

[10] Kadhim, I.J., Premaratne, P., Vial, P.J., Halloran, B. (2017). A comparative analysis among dual tree complex wavelet and other wavelet transforms based on image compression. In Intelligent Computing Theories and Application, pp. 569-580. https://doi.org/10.1007/978-3-319-63312-1_50

[11] Hussain, A.J., Al-Fayadh, A., Radi, N. (2018). Image compression techniques: A survey in lossless and lossy algorithms. Neurocomputing, 300: 44-69. https://doi.org/10.1016/j.neucom.2018.02.094

[12] Ahmed, S.K. (2022). A modified method for selecting singular values in image compression using singular value decomposition. Journal of Engineering Science and Technology, 17(4): 2556-2566.

[13] Al-Obaidi, M.K., Ahmed, A.F. (2022). Implementation of image compression based on singular value decomposition. Global Journal of Engineering and Technology Advances, 11(3): 86-92. https://doi.org/10.30574/gjeta.2022.11.3.0097

[14] Taj, R., Tao, F., Kanwal, S., Almogren, A., Rehman, A.U. (2024). A SURF and SVD-based robust zero-watermarking for medical image integrity. PLOS ONE, 19(9): e0307619. https://doi.org/10.1371/journal.pone.0307619

[15] Kumar, P., Parmar, A. (2020). Versatile approaches for medical image compression: A review. Procedia Computer Science, 167: 1380-1389. https://doi.org/10.1016/j.procs.2020.03.349

[16] Latreche, B., Merrad, A., Benziane, A., Naimi, H., Saadi, S. (2025). A robust dual-layer medical image watermarking scheme based on matrix factorization in the LWT domain for E-healthcare applications. Multimedia Tools and Applications, 84(25): 29883-29913. https://doi.org/10.1007/s11042-024-20331-7

[17] Liu, X., Wu, Y., Gao, P., Ouyang, J., Shao, Z. (2022). Color image watermarking based on singular value decomposition and generalized regression neural network. Multimedia Tools and Applications, 81(22): 32073-32091. https://doi.org/10.1007/s11042-022-12990-1

[18] Sundara Rajan, P.V., Fred, A.L. (2019). An efficient compound image compression using optimal discrete wavelet transform and run length encoding techniques. Journal of Intelligent Systems, 28(1): 87-101. https://doi.org/10.1515/jisys-2016-0096

[19] Asokan, A., Anitha, J., Ciobanu, M., Gabor, A., Naaji, A., Hemanth, D.J. (2020). Image processing techniques for analysis of satellite images for historical maps classification—An overview. Applied Sciences, 10(12): 4207. https://doi.org/10.3390/app10124207

[20] Barbhuiya, A.J.I., Laskar, T.A., Hemachandran, K. (2014). An approach for color image compression of JPEG and PNG images using DCT and DWT. In 2014 International Conference on Computational Intelligence and Communication Networks, Bhopal, India, pp. 129-133. https://doi.org/10.1109/CICN.2014.40

[21] Cho, H., Jeon, S. (2025). Optimization of medical image compression based on singular value decomposition.

SSRN preprint. https://doi.org/10.2139/ssrn.5162906
[22] Abd Gani, S.F., Hamzah, R.A., Latip, R., Salam, S., Noraqillah, F., Herman, A.I. (2022). Image compression using singular value decomposition by extracting red, green, and blue channel colors. Bulletin of Electrical Engineering and Informatics, 11(1): 168-175. https://doi.org/10.11591/eei.v11i1.2602
[23] Hamzah, R.A., Ibrahim, H., Hassan, A.H.A. (2016). Stereo matching algorithm based on illumination control to improve the accuracy. Image Analysis and Stereology, 35(1): 39-52. https://doi.org/10.5566/ias.1369
[24] Hamzah, R.A., Wei, M.G.Y., Anwar, N.S.N. (2019). Stereo matching based on absolute differences for multiple objects detection. Telecommunication Computing Electronics and Control, 17(1): 261-267. https://doi.org/10.12928/TELKOMNIKA.v17i1.9185
[25] Hamzah, R.A., Ibrahim, H. (2018). Improvement of stereo matching algorithm based on sum of gradient magnitude differences and semi-global method with refinement step. Electronics Letters, 54(14): 876-878. https://doi.org/10.1049/el.2017.3956
[26] Kanwal, S., Tao, F., Taj, R., Abbas, Q., Amin, F. (2025). Securing medical images using multi-step watermarking model. Peer-to-Peer Networking and Applications, 18(5): 253. https://doi.org/10.1007/s12083-025-02041-5
[27] Kusuma, M.R., Panggabean, S. (2026). Robust digital image watermarking using DWT, Hessenberg, and SVD for copyright protection. International Journal of Advanced Computing and Informatics, 2(1): 41-52. https://doi.org/10.71129/ijaci.v2i1.pp41-52
[28] Chaudhary, H., Garg, P., Vishwakarma, V.P. (2025). Enhanced medical image watermarking using hybrid DWT-HMD-SVD and Arnold scrambling. Scientific Reports, 15(1): 9710. https://doi.org/10.1038/s41598-025-94080-4
[29] Sahir, M., Bekkouche, T., Belilita, F., Amardjia, N. (2025). An optimized color image watermarking scheme based on HD and SVD in DWT domain. Engineering, Technology & Applied Science Research, 15(2): 21639-21646. https://doi.org/10.48084/etasr.9504
[30] Naveen Kumar, R. (2024). An efficient image compression using modified embedded zero tree coding with SVD. Multimedia Tools and Applications, 83(13): 37795-37812. https://doi.org/10.1007/s11042-023-16725-8
[31] Kumar, R., Patbhaje, U., Kumar, A. (2022). An efficient technique for image compression and quality retrieval using matrix completion. Journal of King Saud University-Computer and Information Sciences, 34(4): 1231-1239. https://doi.org/10.1016/j.jksuci.2019.08.002